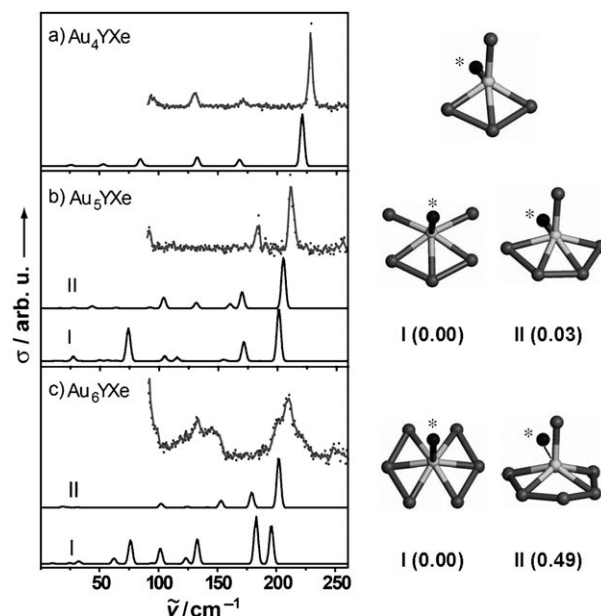


Fluxionality and  $\sigma$ -Aromaticity in Small Yttrium-Doped Gold ClustersLing Lin,<sup>[c]</sup> Tibor Höltzl,<sup>[c]</sup> Philipp Gruene,<sup>[a]</sup> Pieterjan Claes,<sup>[b]</sup> Gerard Meijer,<sup>[a]</sup> André Fielicke,<sup>\*,[a]</sup> Peter Lievens,<sup>\*,[b]</sup> and Minh Tho Nguyen<sup>\*,[c]</sup>

Aromaticity is a qualitative concept which has been applied in organic chemistry very successfully.<sup>[1,2]</sup> Recently, it has been extended to compounds containing different metallic elements.<sup>[3]</sup> Reported examples of aromatic binary clusters of transition metals include the  $\text{Au}_5\text{Zn}^+$  cation<sup>[4]</sup> and the neutral  $\text{Cu}_7\text{Sc}$  molecule.<sup>[5]</sup> In  $\text{Au}_5\text{Zn}^+$ , the six delocalized  $\sigma$ -electrons satisfy the Hückel ( $4n+2$ ) rule, and it is a  $\sigma$ -aromatic five-membered ring.<sup>[4]</sup> The ten  $\sigma$ -electrons in  $\text{Cu}_7\text{Sc}$  are also fully delocalized, and on the basis of electron count and a partition of its electron density, this seven-membered ring was shown to be  $\sigma$ -aromatic.<sup>[5]</sup> We now present experimental evidence for the geometrical structure of the small neutral yttrium-doped gold clusters  $\text{Au}_{4-6}\text{Y}$  in the gas phase, and demonstrate theoretically that the anion  $\text{Au}_6\text{Y}^-$  constitutes a new bimetallic aromatic six-membered cycle.

Structural information on neutral Y-doped Au clusters is obtained by means of vibrational spectroscopy. To record the vibrational spectra of the clusters in the gas phase, we employ the infrared multiple photon dissociation (IR-MPD) technique using action spectroscopy with Xe as the messenger atom.<sup>[6]</sup> The Free Electron Laser for Infrared eXperiments (FELIX) provides intense radiation in the far IR.<sup>[7]</sup> Details are provided in the Supporting Information.

Let us first consider the IR spectroscopic results of the smaller clusters  $\text{Au}_4\text{Y}$  and  $\text{Au}_5\text{Y}$ . Their experimental spectra are displayed in Figures 1a and b together with the calculated vibrational spectra of the Xe complexes. Quantum chemical calculations were carried out using the DFT method with the pure BP86 functional, and the MO coupled-cluster theory CCSD(T) method (computational details and a table with experimental and scaled calculated IR frequencies are given in the Supporting Information).<sup>[8]</sup> An initial calibration of DFT methods points



**Figure 1.** Comparison between calculated and experimental IR-MPD spectra of a)  $\text{Au}_4\text{Y}$ , b)  $\text{Au}_5\text{Y}$ , and c)  $\text{Au}_6\text{Y}$  with one Xe atom (in black with \*) attached. Calculated stick spectra (BP86/cc-pVDZ-PP, lower panels) without using any frequency scaling are folded with a Gaussian line-width function of  $4\text{ cm}^{-1}$  full width at half maximum. The experimental data points are overlaid with a three-point running average to account for the bandwidth of FELIX. Relative energies (BP86/cc-pVDZ-PP) are given in eV.

out that the BP86 functional leads to reliable predictions of the vibrational frequencies for transition-metal-doped clusters.<sup>[9]</sup> Relative energies given hereafter include the zero-point energy corrections. Note that  $\text{Au}_2\text{Y}$  has a slightly bent Au–Y–Au structure ( $C_{2v}$ ) and  $\text{Au}_3\text{Y}$  exhibits a  $D_{3h}$  form in which the Y atom occupies the central position. Attachment of an additional gold atom destroys the high symmetry, giving rise to a non-planar ( $C_s$ )  $\text{Au}_4\text{Y}$  cluster, with a central Y atom but a fourth axial Au atom. The Xe atom prefers to attach to Y in a *trans* position to the fourth Au atom with respect to the central AuY axis. The observed IR spectrum of  $\text{Au}_4\text{Y}$  features an intense peak centred at  $228\text{ cm}^{-1}$ , which is reproduced well by DFT calculations ( $221\text{ cm}^{-1}$ , Figure 1a). Addition of the fifth gold atom leads to two distinct lower-lying  $\text{Au}_5\text{Y}$  forms nearly having the same energy at both BP86 and CCSD(T) levels. While **Au<sub>5</sub>Y-I** is planar ( $C_{2v}$ ), **Au<sub>5</sub>Y-II** still maintains a non-planar  $C_s$  form. In both cases, an attachment of Xe to Y is preferred. The IR spectra of both isomers in the region of  $150\text{--}225\text{ cm}^{-1}$  turn out to be similar, and both compare relatively well with the observed spectrum, whose peaks are centered at  $185$  and  $211\text{ cm}^{-1}$  (Figure 1b). Therefore, the isomers of  $\text{Au}_5\text{Y}$  cannot be discriminated based

[a] P. Gruene, Prof. G. Meijer, Dr. A. Fielicke  
Fritz-Haber-Institut der Max-Planck-Gesellschaft  
Faradayweg 4-6, D-14195 Berlin (Germany)  
Fax: (+49) 30-8413-5603  
E-mail: fielicke@fhi-berlin.mpg.de

[b] P. Claes, Prof. P. Lievens  
Laboratory of Solid State Physics and Magnetism  
and INPAC-Institute for Nanoscale Physics and Chemistry  
University of Leuven, B-3001 Leuven (Belgium)  
Fax: (+32) 16-327983  
E-mail: peter.lievens@fys.kuleuven.be

[c] Dr. L. Lin, T. Höltzl, Prof. M. T. Nguyen  
Department of Chemistry  
and INPAC-Institute for Nanoscale Physics and Chemistry  
University of Leuven, B-3001 Leuven (Belgium)  
Fax: (+32) 16-327992  
E-mail: minh.nguyen@chem.kuleuven.be

Supporting information for this article is available on the WWW under <http://dx.doi.org/10.1002/cphc.200800580>.

on their vibrational spectra alone, and might coexist in the experiment.

The experimental spectrum shown in the upper panel of Figure 1c has been obtained by IR-MPD of the Xe complex of  $\text{Au}_6\text{Y}$ .<sup>[7c]</sup> Among the numerous structures of  $\text{Au}_6\text{Y}$  possessing a doublet ground state, the two shown in Figure 2 are the

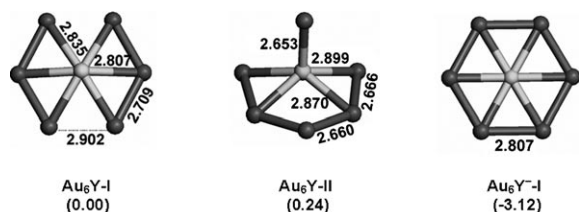


**Figure 2.** BP86/cc-pVDZ-PP structures [bond lengths in Å] of the two lowest-energy neutral isomers  $\text{Au}_6\text{Y-I}$  and  $\text{Au}_6\text{Y-II}$ , and the anion  $\text{Au}_6\text{Y}^-$ . Relative energies given in parentheses [eV] were obtained from CCSD(T)/cc-pVTZ-PP using BP86 geometries.

lowest-lying isomers. Both forms have a Y centre, but are non-planar. A correspondence between  $\text{Au}_6\text{Y-I}$  and  $\text{Au}_6\text{Y-II}$  with  $\text{Au}_5\text{Y-I}$  and  $\text{Au}_5\text{Y-II}$ , respectively, can be established.  $\text{Au}_6\text{Y-II}$  arises from  $\text{Au}_6\text{Y-I}$  by a strong out-of-plane motion of one Au atom. The non-planarity and low-spin state of  $\text{Au}_6\text{Y}$  make it markedly different from other  $\text{Au}_6\text{M}$  clusters with  $\text{M} = \text{Ti}, \text{V}$  and  $\text{Cr}$ .<sup>[10]</sup>  $\text{Au}_6\text{Y-I}$  ( $^2\text{A}_1, \text{C}_{2v}$ ) is more stable than  $\text{Au}_6\text{Y-II}$  ( $^2\text{A}''', \text{C}_3$ ) by 0.24 eV with CCSD(T) and 0.35 eV with BP86 calculations.

For  $\text{Au}_6\text{Y}$ , the Xe atom also prefers to attach to Y, and the same energy ordering of the two isomers is also found for Xe complexes, but the energy difference between them is increased to 0.49 eV (BP86). Figure 1c compares the calculated and observed IR spectra of Xe complexes of the two lowest  $\text{Au}_6\text{Y}$  isomers. Interestingly, the experimental IR spectrum is characterized by unusually broad bands—much broader than observed for  $\text{Au}_4\text{Y}$  and  $\text{Au}_5\text{Y}$ —which are not reproduced in the calculated spectra of  $\text{Au}_6\text{Y-I-Xe}$  and  $\text{Au}_6\text{Y-II-Xe}$ .

We now consider the IR spectrum of the lower-lying  $\text{Au}_6\text{Y-I-Xe}$ . The Y–Xe stretch vibration corresponds to a peak at  $76 \text{ cm}^{-1}$ , which seemingly corresponds to the observed outermost left band. The observed band ranging from  $100$  to  $150 \text{ cm}^{-1}$  is attributed to Au–Au and Y–Au stretch vibrations. The observed band at  $\sim 200 \text{ cm}^{-1}$  is a combination of two Au–Y stretch modes, one calculated at  $183$  and the other at  $196 \text{ cm}^{-1}$ . The observed strong broadening of the IR bands of  $\text{Au}_6\text{Y}$  needs further consideration. A rationalization would be to attribute this observation to a size-specific highly fluxional character. Indeed, broadening of vibrational bands of various species has been discussed before in terms of very rapid rearrangements. In the case of tricarbonyl ( $\eta^4$ -norbornadiene) iron, fast interwell dynamical processes have been invoked.<sup>[11]</sup> For the methonium cation  $\text{CH}_5^+$  large-amplitude vibrations observed as broad features in the infrared spectrum have been explained through a dynamical mechanism for hydrogen exchange and eventually full hydrogen scrambling.<sup>[12]</sup> Also for Si and Au clusters fluxional characteristics have been described for specific sizes.<sup>[13]</sup> In the present case, as is illustrated in the

potential energy curves shown in Figure 3, the neutral  $\text{Au}_6\text{Y-I}$  species is highly fluxional; it distorts along different axes extremely easily. In fact, the barrier of inversion through a planar transition structure (Figure 3a) amounts to only  $1.9 \text{ kJ mol}^{-1}$

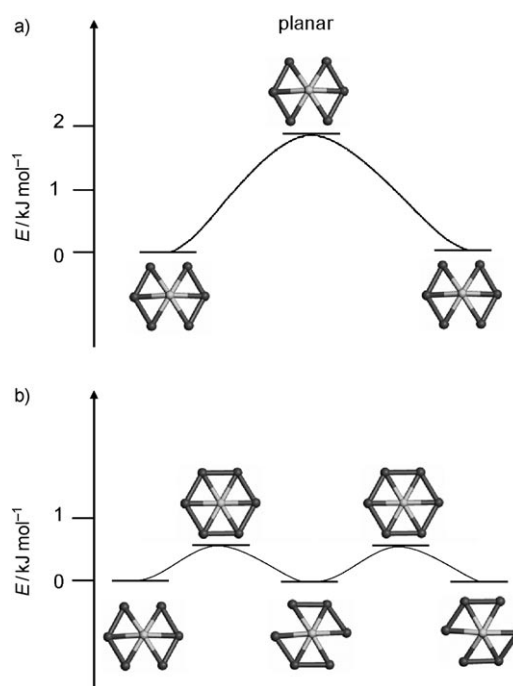


**Figure 3.** Potential energy curves corresponding to a) the inversion, and b) the bond stretching isomerization of the neutral  $\text{Au}_6\text{Y-I}$  obtained at the BP86/cc-pVDZ-PP level.

(BP86 level). More interestingly, the bond stretching isomerization (Figure 3b) is also a highly facile process, as the corresponding energy barrier amounts to only  $\sim 0.5 \text{ kJ mol}^{-1}$  at the same level. The existence of the different bond stretching isomers is a consequence of the partially filled quasi-degenerate SOMO and SOMO–1 orbitals. In  $D_{6h}$  symmetry these orbitals are perfectly degenerate, which then yield the three bond-stretching isomers by Jahn–Teller distortions. This highly anharmonic potential with several degenerate minima in the PES separated by very low barriers is expected to yield fluxional behaviour of the cluster on picosecond timescales, which in turn would explain the broadening of the IR peaks of  $\text{Au}_6\text{Y}$ . Such a broadening was not observed for  $\text{Au}_4\text{Y}$  and  $\text{Au}_5\text{Y}$ , which do not possess similar electronic structures.

Overall, the good agreement for  $\text{Au}_4\text{Y}$  and  $\text{Au}_5\text{Y}$  (Figures 1a–b), and the relatively good agreement for  $\text{Au}_6\text{Y}$  (Figure 1c), taking into account the fluxionality-induced broadening, provides structural identification of the neutral  $\text{Au}_6\text{Y}$  cluster.

The observed structure of  $\text{Au}_6\text{Y}$  can be understood based on its electronic structure. According to the phenomenological shell model,<sup>[14]</sup> MOs composed of the valence s orbitals determine the properties and electronic structure of alkaline and metallic clusters such as  $\text{Cu}_7\text{Sc}$  to a great extent.<sup>[5]</sup> In planar (nearly) cylindrical clusters, shell closing occurs at ten electrons, which correspond to the  $(1s)^2(1p_x)^2(1p_y)^2(1d_{xy})^2(1d_{x^2-y^2})^2$  con-

figuration.<sup>[15]</sup> The partial density of states (DOS) of **Au<sub>6</sub>Y-I** indicates that other MOs with large contributions from s orbitals exist. Together with the three electrons of Y, **Au<sub>6</sub>Y-I** has nine electrons in the shell model MOs. The electron localization indicator (ELI-D)<sup>[16]</sup> isosurface of **Au<sub>6</sub>Y-I**, given in Figure 4 a, dem-

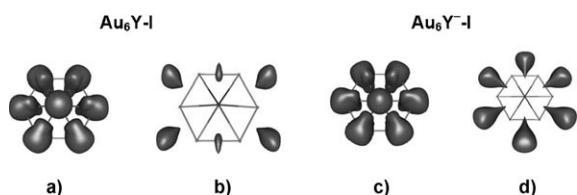


**Figure 4.** ELI-D isosurfaces for a) **Au<sub>6</sub>Y-I** and c) **Au<sub>6</sub>Y<sup>-I</sup>** (isovalues = 1.3). Partial ELI-D computed from MOs corresponding to the phenomenological shell model of b) **Au<sub>6</sub>Y-I** and d) **Au<sub>6</sub>Y<sup>-I</sup>**.

onstrates that there are localization domains only around the nuclei. The partial ELI-D function for the shell model MOs of **Au<sub>6</sub>Y-I** (Figure 4b) is similar to the result for **Cu<sub>7</sub>Sc**,<sup>[5]</sup> which thus suggests that MOs with high contributions from valence s orbitals are mainly responsible for the chemical bonding in these clusters. The ELI-D function is much less important in the longer Au–Au bonds, suggesting that the electron distribution in these MOs is responsible for the elongation of these distances.

Attachment of an extra electron to the neutral cluster **Au<sub>6</sub>Y-I** yields the anion **Au<sub>6</sub>Y<sup>-I</sup>** (Figure 2). Figure 5 shows the total and partial DOS of the s orbitals of the anion **Au<sub>6</sub>Y<sup>-I</sup>**, where the MOs corresponding to the shell model are also assigned. **Au<sub>6</sub>Y<sup>-I</sup>** behaves like a 10-electron system satisfying both the shell model and Hückel's rule. Such an electronic configuration belongs to a perfect six-membered ring shape, and induces a

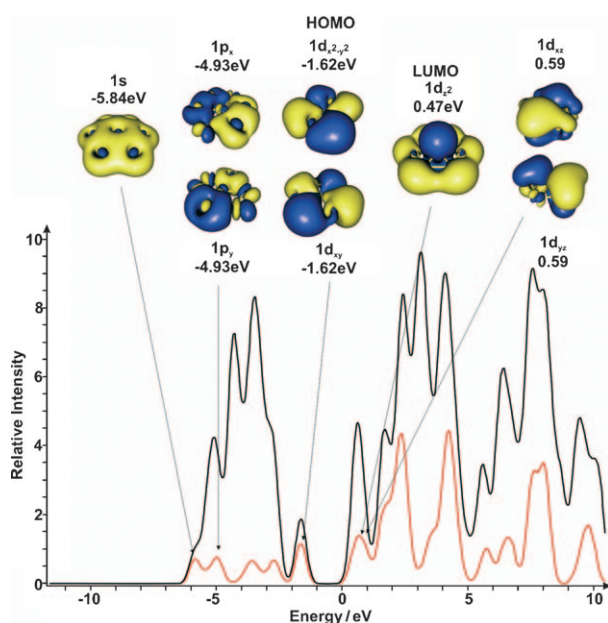


**Figure 5.** Total (black) and partial (computed from the s AOs, red) density of states and shell model MOs of the **Au<sub>6</sub>Y<sup>-I</sup>** anion having high contributions from 6s AOs of Au, and 5s AO of Y.

strong stabilization effect. Indeed, **Au<sub>6</sub>Y<sup>-I</sup>** is calculated to have a planar  $D_{6h}$  symmetry and exhibits a particularly strong binding of the extra electron. The electron affinity of **Au<sub>6</sub>Y-I** amounts to 3.12 eV (Figure 2). The HOMO–LUMO gap of 2.07 eV for **Au<sub>6</sub>Y<sup>-I</sup>** is comparable to that of, for example, **Au<sub>14</sub>Sc<sup>-</sup>**.<sup>[17]</sup> Both calculated energetic parameters suggest a high stability of the **Au<sub>6</sub>Y<sup>-I</sup>** anion. Consistently, as shown in Figure 4 d, there are equivalent domains for **Au<sub>6</sub>Y<sup>-I</sup>** in the partial ELI-D function for the shell model MOs.

To probe the electronic behaviour of the anion further, the nucleus-independent chemical shifts (NICS)<sup>[2,18]</sup> were calculated. Since the NICS(0) value is strongly influenced by core electrons of the atom in the center of the ring, we rather used the NICS(1) and NICS(2) values where the ghost atom is put 1.0 and 2.0 Å above the middle of the ring, respectively. The NICS(1) value computed above the center of the ring of -15.3 ppm for **Au<sub>6</sub>Y<sup>-I</sup>** can be compared to the corresponding value previously calculated for **Cu<sub>7</sub>Sc**.<sup>[5]</sup> The NICS(2) value at the center of the three-membered Au–Y–Au rings (about -6.5 ppm) of this cluster can be compared to the previously reported value of about -5 ppm for the  $\sigma$ -aromatic five-membered cyclic cation **Au<sub>5</sub>Zn<sup>+</sup>** ( $D_{5h}$ ).<sup>[4]</sup> The distribution of NICS(1), NICS(2) and the corresponding zz tensor are negative for **Au<sub>6</sub>Y<sup>-I</sup>**, thus lending further support for the aromatic character of the anion. Moreover, the NICS(1) and NICS(1)<sub>zz</sub> of **Au<sub>6</sub>Y<sup>-I</sup>** are calculated to be more negative than NICS(2) and NICS(2)<sub>zz</sub>, which is an additional indication for its  $\sigma$ -aromaticity (cf. ESI).

In summary, we report the IR spectra of **Au<sub>4</sub>Y**, **Au<sub>5</sub>Y**, and **Au<sub>6</sub>Y**, which represent the first experimental far-IR spectroscopic data on neutral doped metal clusters in the gas phase. Comparisons with DFT/BP86 calculations allow their ground state structures to be identified. Calculations show that the global minimum of **Au<sub>6</sub>Y** possesses a non-planar  $C_{2v}$  structure, while the highly fluxional behaviour of this structure accounts for the experimentally observed line broadening in the IR spectra.

The corresponding anion **Au<sub>6</sub>Y<sup>-</sup>** has a planar cyclic  $D_{6h}$  form and the distribution of its  $\sigma$  electrons complies with the electronic shell model. The anion is relatively stable with respect to electron detachment ( $I E_a = 3.1 \pm 0.1$  eV). The stability, high symmetry, closed electronic structure and the magnetic properties suggest that it can be regarded as a new  $\sigma$ -aromatic six-membered all-metallic cycle. Its experimental characterization is envisaged by, among others, photoelectron spectroscopy-based techniques.

## Acknowledgements

The Leuven groups are indebted to the FWO-Vlaanderen and the K. U. Leuven Research Council. P.C. thanks the IWT-Vlaanderen. P.G. thanks the IMPRS "Complex Surfaces in Materials Science" for funding. This work is supported by the Stichting voor Fundamenteel Onderzoek der Materie (FOM) in providing beam time for FELIX, and by the European Community-Research Infrastructure Action under the FP6 "Structuring the European Research Area" Programme (through the Integrated Infrastructure Initiative "Integrating Activity on Synchrotron and Free Electron Laser Science").

**Keywords:** aromaticity · cluster compounds · gold · IR-MPD spectroscopy · yttrium

- [1] a) P. J. Garratt, *Aromaticity*, Wiley, New York, **1986**; b) V. I. Minkin, M. N. Glukhovtsev, B. Y. Simkin, *Aromaticity and Antiaromaticity*, Wiley, New York, **1994**.
- [2] Z. Chen, C. S. Wannere, C. Corminboeuf, R. Puchta, P. v. R. Schleyer, *Chem. Rev.* **2005**, *105*, 3842.
- [3] For a recent reference, see D. Y. Zubarev, B. B. Averkiev, H. J. Zhai, L. S. Wang, A. I. Boldyrev, *Phys. Chem. Chem. Phys.* **2008**, *10*, 257.
- [4] H. Tanaka, S. Neukermans, E. Janssens, R. E. Silverans, P. Lievens, *J. Am. Chem. Soc.* **2003**, *125*, 2862.
- [5] T. Höltzl, E. Janssens, N. Veldeman, T. Veszprémi, P. Lievens, M. T. Nguyen, *ChemPhysChem* **2008**, *9*, 833.
- [6] A. Fielicke, A. Kirilyuk, C. Ratsch, J. Behler, M. Scheffler, G. von Helden, G. Meijer, *Phys. Rev. Lett.* **2004**, *93*, 023401.
- [7] a) G. von Helden, D. van Heijnsbergen, G. Meijer, *J. Phys. Chem. A* **2003**, *107*, 1671; b) A. Fielicke, G. von Helden, G. Meijer, *Eur. Phys. J. D* **2005**, *34*, 83; c) Details of IR-MPD experiments are given in the Supporting Information.
- [8] M. J. Frisch, G. W. Trucks, H. B. Schlegel, G. E. Scuseria, M. A. Robb, J. R. Cheeseman, J. A. Montgomery, Jr., T. Vreven, K. N. Kudin, J. C. Burant, J. M. Millam, S. S. Iyengar, J. Tomasi, V. Barone, B. Mennucci, M. Cossi, G. Scalmani, N. Rega, G. A. Petersson, H. Nakatsuji, M. Hada, M. Ehara, K. Toyota, R. Fukuda, J. Hasegawa, M. Ishida, T. Nakajima, Y. Honda, O. Kitao, H. Nakai, M. Klene, X. Li, J. E. Knox, H. P. Hratchian, J. B. Cross, V. Bakken, C. Adamo, J. Jaramillo, R. Gomperts, R. E. Stratmann, O. Yazyev, A. J. Austin, R. Cammi, C. Pomelli, J. W. Ochterski, P. Y. Ayala, K. Morokuma, G. A. Voth, P. Salvador, J. J. Dannenberg, V. G. Zakrzewski, S. Dapprich, A. D. Daniels, M. C. Strain, O. Farkas, D. K. Malick, A. D. Rabuck, K. Raghavachari, J. B. Foresman, J. V. Ortiz, Q. Cui, A. G. Baboul, S. Clifford, J. Cioslowski, B. B. Stefanov, G. Liu, A. Liashenko, P. Piskorz, I. Komaromi, R. L. Martin, D. J. Fox, T. Keith, M. A. Al-Laham, C. Y. Peng, A. Nanayakkara, M. Challacombe, P. M. W. Gill, B. Johnson, W. Chen, M. W. Wong, C. Gonzalez, J. A. Pople, *Gaussian 03, Revision C.02*, Gaussian, Inc., Wallingford CT, **2004**.
- [9] P. Gruene, A. Fielicke, G. Meijer, E. Janssens, V. T. Ngan, M. T. Nguyen, P. Lievens, *ChemPhysChem* **2008**, *9*, 703.
- [10] X. Li, B. Kiran, L. F. Cui, L. S. Wang, *Phys. Rev. Lett.* **2005**, *95*, 253401.
- [11] a) F. W. Grevels, J. Jacke, W. E. Klotzbücher, C. Krüger, K. Seevogel, Y. H. Tsay, *Angew. Chem.* **1987**, *99*, 960; *Angew. Chem. Int. Ed. Engl.* **1987**, *26*, 885; b) J. J. Turner, C. M. Gordon, S. M. Howdle, *J. Phys. Chem.* **1995**, *99*, 17532; c) J. J. Turner, F. W. Grevels, S. M. Howdle, J. Jacke, M. T. Howard, W. E. Klotzbücher, *J. Am. Chem. Soc.* **1991**, *113*, 8347; d) C. H. Londergan, C. P. Kubiak, *Chem. Eur. J.* **2003**, *9*, 5962.
- [12] a) E. T. White, J. Tang, T. Oka, *Science* **1999**, *284*, 135; b) O. Asvany, P. Kumar, B. Redlich, I. Hegemann, S. Schlemmer, D. Marx, *Science* **2005**, *309*, 1219; c) X. Huang, A. B. McCoy, J. M. Bowman, L. M. Johnson, C. Savage, F. Dong, D. J. Nesbitt, *Science* **2006**, *311*, 60.
- [13] a) A. D. Zdetsis, *J. Chem. Phys.* **2007**, *127*, 014314; b) X. Gu, S. Bulusu, X. Li, X. C. Zeng, J. Li, X. G. Gong, L. S. Wang, *J. Phys. Chem. C* **2007**, *111*, 8228.
- [14] a) W. A. de Heer, *Rev. Mod. Phys.* **1993**, *65*, 611; b) I. Katakuse, T. Ichihara, Y. Fujita, T. Matsuo, T. Sakurai, H. Matsuda, *Int. J. Mass Spectrom. Ion Process.* **1985**, *67*, 229; c) E. Janssens, S. Neukermans, P. Lievens, *Curr. Opin. Solid State Mater. Sci.* **2004**, *8*, 185.
- [15] E. Janssens, H. Tanaka, S. Neukermans, R. E. Silverans, P. Lievens, *New J. Phys.* **2003**, *5*, 46.
- [16] a) M. Kohout, F. R. Wagner, Y. Grin, *Int. J. Quantum Chem.* **2006**, *106*, 1499; b) F. R. Wagner, V. Bezugly, M. Kohout, Y. Grin, *Chem. Eur. J.* **2007**, *13*, 5724.
- [17] Y. Gao, S. Bulusu, X. C. Zeng, *J. Am. Chem. Soc.* **2005**, *127*, 15680.
- [18] P. v. R. Schleyer, C. Maerker, A. Dransfeld, H. Jiao, N. J. R. van Eikema Hommes, *J. Am. Chem. Soc.* **1996**, *118*, 6317.

Received: September 3, 2008

Published online on November 12, 2008